JOURNAL OF MATERIALS SCIENCE 28 (1993) 547–552

# Decomposition of $CO_2$ and CO into carbon with active wüstite prepared from Zn(II)-bearing ferrite

T. KODAMA, M. TABATA, K. TOMINAGA, T. YOSHIDA, Y. TAMAURA
*Department of Chemistry, Tokyo Institute of Technology, Meguro-ku, Tokyo 152, Japan*

$CO_2$ decomposition reaction into carbon was studied at 300 °C using the $H_2$-reduced Zn(II)-bearing ferrite which consisted of the Zn(II) oxide and the active wüstite. The $H_2$-reduced Zn(II)-bearing ferrite was prepared from Zn(II)-bearing ferrite by the reduction with $H_2$ gas at 300 °C. The wüstite ($Fe_\delta O$) in the $H_2$-reduced Zn(II)-bearing ferrite had a higher $\delta$ value ($\delta = 0.97$, active wüstite) than those of the normal wüstites ($0.90 < \delta < 0.95$) prepared at high temperatures ($> 570$ °C). The decomposition reaction of $CO_2$ proceeds in two steps: (1) $CO_2$ reduction to CO, and (2) CO decomposition into carbon. In the initial stage, the reduction of $CO_2$ into CO takes place, accompanying both the oxidation of the active wüstite to the slightly oxidized wüstite, and the transformation of active wüstite and Zn(II) oxide into the Zn(II)-bearing ferrite. After the reaction of the initial stage attains equilibrium of an apparent state of rest, the adsorbed CO is decomposed into carbon, associated with the transformation of the slightly oxidized wüstite and the Zn(II) oxide into the Zn(II)-bearing ferrite.

## 1. Introduction

The reduction of $CO_2$ to CO, and hydrocarbons such as $CH_4$, $CH_3OH$ or CHOOH by electrochemical, photoelectrocatalytic, and catalytic reactions, has been studied by many investigators [1–10]. However, studies on the decomposition of $CO_2$ into carbon are very limited. Sacco and Reid [11] studied the decomposition of the $CO_2$ gas with $H_2$ using metallic iron as the catalyst (Bosch reaction). They reported the deposition of carbon on the surface of the iron catalyst during the reaction at 527–627 °C; metallic iron decomposed $CO_2$ gas into carbon in the presence of $H_2$ gas at high temperatures, and the iron oxides (magnetite and wüstite) were formed in the iron catalyst during the reaction. Sacco and Reid concluded that the metallic iron was oxidized by $H_2O$ formed by the hydrogenation of $CO_2$ with $H_2$; the hydrogenation of $CO_2$ simultaneously takes place by the catalytic reaction of the metallic iron, which produces $H_2O$. Lee *et al.* [12] found that the metallic iron was progressively transformed into a mixture of iron oxide (magnetite) and carbides during the course of the decomposition reaction of $CO_2$ gas with $H_2$ using metallic iron. Thus, the decomposition of $CO_2$ into carbon with metallic iron in the presence of $H_2$ gas was accompanied by side reactions such as the hydrogenation of the $CO_2$ and the formation of the carbides. Decomposition of the $CO_2$ gas with metals in the absence of $H_2$ gas has been studied for some alkaline-earth metals such as calcium, strontium and barium. These alkaline-earth metals can decompose $CO_2$ into carbon at elevated temperatures, accompanied by metal oxidation and the formation of carbides [13]. These reports show that the $CO_2$ gas is decomposed into carbon by the incorporation of oxygen from $CO_2$ with metals. These investigations were concerned with the decomposition of $CO_2$ into carbon with metals. However, there have been no reports on the decomposition reaction of the $CO_2$ gas into carbon with metal oxides.

This paper presents the decomposition of the $CO_2$ and CO gases into carbon at 300 °C with the $H_2$-reduced Zn(II)-bearing ferrite which consists of the metal oxides of wüstite and Zn(II) oxide.

## 2. Experimental procedure

### 2.1. Preparation of Zn(II)-bearing ferrite

Zn(II)-bearing ferrite was synthesized by air oxidation of aqueous suspensions of Fe(II) hydroxide and Zn(II) ions [14]. After passing nitrogen gas through distilled water (4.0 $dm^3$) for a few hours, $FeSO_4 \cdot 7H_2O$ (300 g) and $ZnSO_4 \cdot 7H_2O$ (151 g) were added. The pH of the solution was adjusted to 10 by adding a 3.0 mol $dm^{-3}$ NaOH solution. Air was passed through the alkaline suspension at 65 °C for 24 h. The reaction pH was kept constant at 10 by adding the 3.0 mol $dm^{-3}$ NaOH solution. The product precipitated was collected by decantation. After washing with acetate-buffered solution, distilled water, and acetone successively, the product was dried in a nitrogen gas stream. The product was identified by X-ray diffractometry with $FeK_\alpha$ radiation (Model RAD-2A diffractometer, Rigaku). The chemical composition of the product was determined by atomic absorption spectroscopy for analysis of the Zn(II) and $Fe_{total}$ contents, and by calorimetry

0022–2461 

with 2,2′-bipyridine for the Fe(II) and $Fe_{total}$ content [15].

### 2.2. Preparation of the $H_2$-reduced Zn(II)-bearing ferrite

The Zn(II)-bearing ferrite (4.0 g) was placed in a quartz tube in the reaction cell (diameter 24 mm × 350 mm). The reaction cell was evacuated, and then placed in the electric furnace and the temperature was raised to 300 °C. After reaching 300 °C, $H_2$ gas was passed through the Zn(II)-bearing ferrite (0.20 $dm^3$ $min^{-1}$) in the reaction cell for 12 h at 300 °C. After the $H_2$-reduction process, the sample was quenched by quickly placing the reaction cell into the refrigerant of ice/NaCl while passing nitrogen gas through the reaction cell. The sample was taken out under a nitrogen atmosphere, and subjected to X-ray diffractometry whilst protecting it from oxidation.

### 2.3. Reaction between the $H_2$-reduced Zn(II)-bearing ferrite, and $CO_2$ or CO gas

After the $H_2$-reduction process, the reaction cell was evacuated and then the desired volume of the $CO_2$ or CO gas was introduced into the reaction cell which was then closed (zero time of the reaction). The internal pressure of the reaction cell was measured using a pressure gauge. The inner gas species were detected by the gas chromatography (Shimadzu GC-8A). The solid samples after the reaction were quenched by quickly placing the reaction cell into the refrigerant of ice/NaCl whilst passing nitrogen gas through the reaction cell. The solid samples were taken out under a nitrogen atmosphere, and subjected to X-ray diffractometry whilst protecting them from oxidation. The carbon deposited on the samples was collected by filtration after dissolving the samples in HCl solutions, and its amount was measured using an elemental carbon analyser (Perkin–Elmer 2400 CHN analyser).

## 3. Results and discussion

Fig. 1 shows the X-ray diffraction (XRD) patterns of the Zn(II)-bearing ferrite ($Zn_{0.95}Fe_{2.04}O_{4.00}$) (Fig. 1a) and the solid product (Fig. 1b) obtained by passing $H_2$ gas through the Zn(II)-bearing ferrite for 12 h at 300 °C. In Fig. 1a, only the peaks corresponding to spinel-type compound are observed. In Fig. 1b, the peaks of the spinel-type structure of the Zn(II)-bearing ferrite disappear and peaks corresponding to Zn(II) oxide and wüstite appear.These results suggest that the Zn(II)-bearing ferrite was completely decomposed into the Zn(II) oxide and wüstite during 12 h $H_2$-reduction of the Zn(II)-bearing ferrite at 300 °C. Thus, $H_2$-reduced Zn(II)-bearing ferrite consists of mainly two phases: the Zn(II) oxide and wüstite. The lattice constant of the wüstite ($a_0$ = 0.4319 nm) was larger than those of the wüstites reported to be prepared at high temperatures (> 570 °C, normal wüstite) [16–18]. This suggests that the wüstite prepared here at 300 °C has a higher δ value ($Fe_\delta O$: δ = 0.97) than those of the normal wüstites

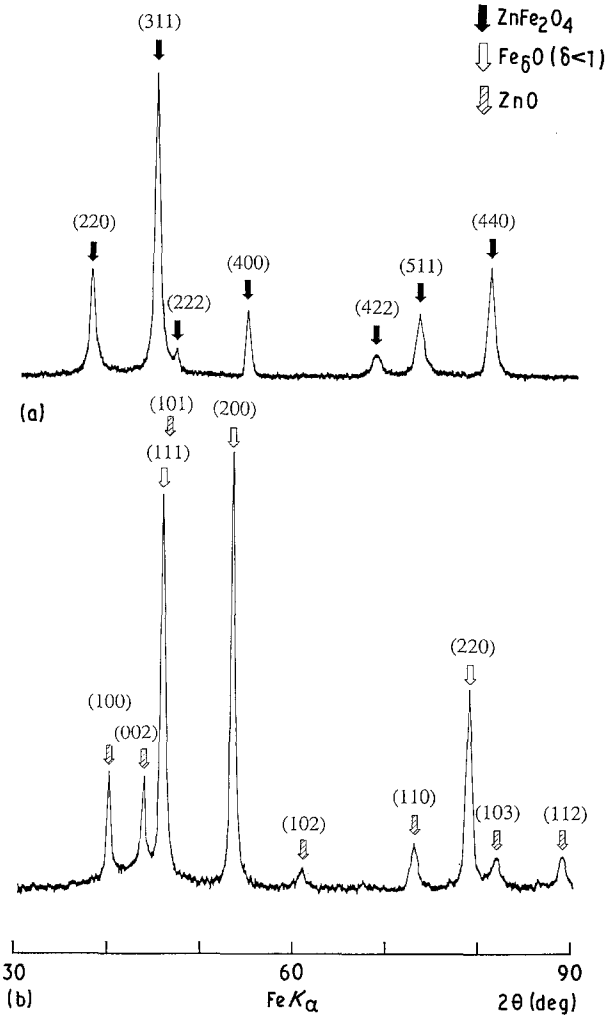


*Figure 1* X-ray diffraction patterns of (a) the Zn(II)-bearing ferrite prepared by air oxidation of aqueous suspensions of Fe(II) hydroxide and Zn(II) ions, and (b) $H_2$-reduced Zn(II)-bearing ferrite prepared by $H_2$ reduction for 12 h at 300 °C.

(0.90 < δ < 0.95). Hereafter, we call the wüstite with a higher δ value, the "active wüstite".

### 3.1. Decomposition reaction of $CO_2$ into carbon with $H_2$-reduced Zn(II)-bearing ferrite

Fig. 2a shows the time variations of the $CO_2$ and CO gas contents during the reaction between $H_2$-reduced Zn(II)-bearing ferrite and $CO_2$ gas at 300 °C (the $CO_2$ decomposition reaction). The initial $CO_2$ gas content in the reaction cell was 100 kPa. As seen from Curve A, the $CO_2$ content rapidly decreased from about 100 kPa to 50 kPa in 4 h during the initial stage of the reaction time. This lowering in the $CO_2$ content was accompanied by the rapid evolution of CO gas in the 4 h, as shown by Curve B. Nearly the same volume of CO gas was rapidly evolved as that of the $CO_2$ gas decreased during the initial stage of the reaction. This indicates that the $CO_2$ gas reacted with the $H_2$-reduced Zn(II)-bearing ferrite and was reduced to CO gas in the initial stage. As can be seen from Curves A and B, both the rapid $CO_2$ decrease and the rapid CO evolution processes apparently ceased after 4 h of the initial stage of the reaction, where the gas content ratio of $CO_2$ to CO is about 1:1. This suggests that the

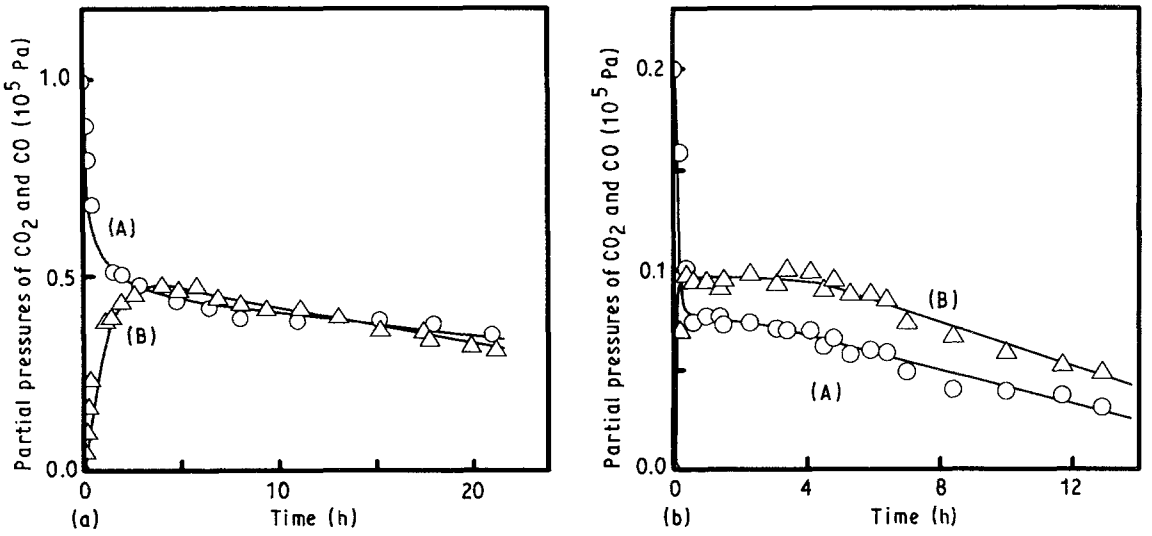


*Figure 2* Variations in the gas contents of (A) $CO_2$, and (B) CO in the reaction cell as a function of reaction time between $H_2$-reduced Zn(II)-bearing ferrite and $CO_2$ gas at 300 °C. The initial $CO_2$ gas content in the reaction cell was (a) 100 kPa and (b) 20 kPa at 300 °C.

reaction of $H_2$-reduced Zn(II)-bearing ferrite with $CO_2$ gas attains equilibrium of an apparent state of rest between the gas phase of $CO_2$ and CO, and the solid phase. This equilibrium reaction may be written

$$CO_2 \rightleftharpoons CO + (O^{2-}) \quad (1)$$

where $(O^{2-})$ denotes oxygen in the solid phase as lattice oxygen. In practice, the adsorbed species would be involved in Equation 1, therefore the reaction will proceed successively, as given by the following equations

$$CO_2 \rightleftharpoons CO_2(ads) \quad (2)$$

$$CO_2(ads) \rightleftharpoons CO(ads) + (O^{2-}) \quad (3)$$

$$CO(ads) \rightleftharpoons CO \quad (4)$$

where $CO_2$(ads) and CO(ads) denote $CO_2$ and CO species adsorbed on the reactive site, respectively. From Fig. 2a, the amount of $CO_2$ gas reduced to CO in the initial stage was about $1.34 \times 10^{-3}$ mol ($pCO_2$ = 50 kPa at 300 °C).

Fig. 2b shows the variation with time of the $CO_2$ and CO contents in the reaction cell during the reaction between $H_2$-reduced Zn(II)-bearing ferrite and $CO_2$ gas at 300 °C, where the lower volume of $CO_2$ gas ($6.13 \times 10^{-4}$ mol, $pCO_2$ = 20 kPa at 300 °C) was initially introduced into the reaction cell. This volume of $CO_2$ gas introduced here (Fig. 2b) is smaller than that of the $CO_2$ gas reduced to CO in the initial stage $1.34 \times 10^{-3}$ mol, $pCO_2$ = 50 kPa at 300 °C) of Fig. 2a. In the experiment of Fig. 2b, we used the same amount of solid phase ($H_2$-reduced Zn(II)-bearing ferrite) as that used in Fig. 2a, therefore the reactive site number is considered to be equal between Fig. 2a and b. If cessation of the rapid $CO_2$ decrease and rapid CO evolution processes during the 4 h of the initial stage of the reaction in Fig. 2a is caused by the consumption of the reactive sites on the surface of the solid phase, the $CO_2$ gas initially introduced in Fig. 2b should all be reduced to CO gas, because the reactive site number is sufficiently large compared with the volume of the $CO_2$ gas introduced in Fig. 2b. However, as can be seen in Fig. 2b, the $CO_2$ gas rapidly decreased, but not all of the $CO_2$ gas was reduced to CO (Curve A). Both the rapid $CO_2$ decrease (Curve A) and the rapid CO evolution (Curve B) processes apparently ceased after 1 h of the initial stage of the reaction, where the gas content ratio of $CO_2$ to CO is about 0.8:1. The volume of $CO_2$ gas reduced to CO ($3.07 \times 10^{-4}$ mol, $pCO_2$ = 10 kPa at 300 °C) in the initial stage of the reaction in Fig. 2b was smaller than that in Fig. 2a ($1.34 \times 10^{-3}$ mol, $pCO_2$ = 50 kPa at 300 °C). These results indicate that the reaction in the initial stage of the $CO_2$ decomposition reaction with the $H_2$-reduced Zn(II)-bearing ferrite is the equilibrium reaction of the solid phase with the $CO_2$ and CO gases given by Equation 1.

As can be seen from Curves A and B in Fig. 2a and b, in the second stage after the initial stage of the reaction, both the $CO_2$ and CO gas contents gradually decreased. During this decrease, the internal pressure of the reaction cell also gradually decreased. The sum of the partial pressures of the $CO_2$ and CO gases was nearly equal to the internal pressure; no other gases, such as $CH_4$ and $C_2H_6$, were detected, except for $CO_2$ and CO by gas chromatography. From these results, it was considered that $CO_2$ or CO gas was gradually decomposed into carbon, and that the oxygen in the $CO_2$ or CO gas was incorporated into the solid phase. It is remarkable that the gas content ratio of $CO_2$ to CO is kept nearly constant at 0.8:1 during decreasing of the $CO_2$ and CO gases (the second stage) in Fig. 2b. The equilibrium constant of Equation 1 is represented by

$$K_p = [pCO_2]/[pCO][(O^{2-})] \quad (5)$$

where $[(O^{2-})]$ denotes the oxygen activity of the solid phase. The oxygen activity of the solid phase changes as the oxygen is incorporated into the solid phase from the $CO_2$ or CO gas. After attaining equilibrium of the apparent state of rest in the initial stage, the equilibrium in the second stage will be set up under a constant oxygen activity of the solid phase, because the amount of solid phase is sufficiently large compared with the volume of $CO_2$ and CO gases reacted during the second stage in Fig. 2b. Therefore, the

oxygen activity of the solid phase in the second stage can be assumed to be kept constant. Then, the Equation 5 will be rewritten as

$$[pCO_2]/[pCO] = K_p[(O^{2-})] = \text{constant} \quad (6)$$

Equation 6 indicates that the gas content ratio of $CO_2$ to CO is kept nearly constant during the second stage of the $CO_2$ decomposition reaction into carbon.

After 22 h reaction, the internal pressure of the reaction cell decreased to almost zero ($pCO_2 = 0.7$ kPa, and $pCO = 0.7$ kPa at 300 °C). The chemical analysis of the carbon deposited on the solid phase showed that at 22 h reaction time it was about 50% of the carbon of the $CO_2$ gas initially present in the reaction cell. This amount of deposited carbon was larger than that estimated from the diminished $CO_2$ volume in the second stage (40%). However, amount of carbon estimated from the diminished CO volume in the second stage (50%) was nearly equal to that from the chemical analysis. If we assume that the adsorbed $CO_2$ is directly decomposed into carbon in the second stage of the $CO_2$ decomposition reaction according to

$$CO_2(ads) \rightarrow C + 2(O^{2-}) \quad (7)$$

the reverse reaction of Equation 3 (oxidation of the absorbed CO into adsorbed $CO_2$) should proceed during the $CO_2$ decomposition reaction, because the adsorbed $CO_2$ will be consumed for the decomposition reaction into carbon (Equation 7). Therefore, Equation 7 will proceed, accompanying the $CO(ad) \rightarrow CO_2(ad)$ reaction. Thus the solid phase is reduced by the reverse reaction of Equation 3 during direct decomposition of $CO_2$ into carbon (Equation 7. However, from the results of the XRD pattern (Fig. 3), reduction of the solid phase did not proceed during the second stage of the $CO_2$ decomposition reaction. Thus, in the second stage of the $CO_2$ decomposition reaction, it would be reasonable to conclude that $CO_2$ is not directly decomposed into carbon, but rather into CO, and then decomposed into carbon. In practice, the adsorbed CO will be decomposed into carbon, as given by

$$CO(ad) \rightarrow C + (O^{2-}) \quad (8)$$

The remaining 50% of the $CO_2$ gas, which was not deposited as carbon, would be present in the forms of $CO_2$ and CO adsorbed on the surface of the solid phase.

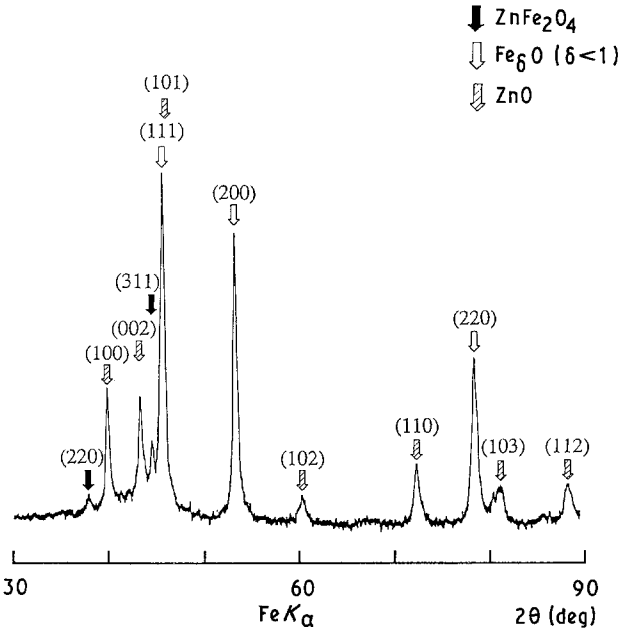


*Figure 3* X-ray diffraction pattern of the solid phase at 22 h reaction time between $H_2$-reduced Zn(II)-bearing ferrite and $CO_2$ gas at 300 °C. The initial $CO_2$ gas content in the reaction cell was 20 kPa at 300 °C.

In the XRD pattern of the solid phase in the initial stage (1 h reaction time in Fig. 2b), small peaks of the spinel-type compound appeared together with peaks of wüstite and Zn(II) oxide. This indicates that wüstite and Zn(II) oxide are transformed into the spinel-type compound during $CO_2$ decomposition. Moreover, it was observed that the lattice constant of the active wüstite decreased from 0.4319 nm to 0.4311 nm. These results suggest that two reactions occur in the solid phase in the initial stage: (1) oxidation of the active wüstite into the slightly oxidized wüstite, and (2) transformation of the active wüstite and Zn(II) oxide into Zn(II)-bearing ferrite. Both of these reactions are accompanied by the incorporation of oxygen from $CO_2$ or CO gas into the solid phase (Equations 3 or 8). From the relationship between the changes in the XRD patterns and those in the $CO_2$ and CO contents in the initial stage, the reduction of $CO_2$ into CO (Equation 3) is considered to be accompanied both by oxidation of the active wüstite into the slightly oxidized wüstite, and by transformation of active wüstite and Zn(II) oxide into Zn(II)-bearing ferrite. The reactions in the initial stage may be represented by the following equations:
in the initial stage

$$Fe_{\delta_1}O + (\delta_1/\delta_2 - 1)CO_2 \rightleftharpoons (\delta_1/\delta_2)Fe_{\delta_2}O + (\delta_1/\delta_2 - 1)CO \quad (\delta_1 > \delta_2) \quad (9)$$

and

$$Fe_\delta O + (\delta/2)ZnO + (3\delta/2 - 1)CO_2 \rightleftharpoons (\delta/2)ZnFe_2O_4 + (3\delta/2 - 1)CO \quad (\delta_1 \geq \delta \geq \delta_2) \quad (10)$$

After the reactions in Equations 9 and 10 attain equilibrium, the adsorbed CO is considered to be gradually decomposed into carbon (Equation 8). Fig. 3 shows the XRD pattern of the solid phase obtained at 22 h after the $CO_2$ decomposition reaction, which is given in Fig. 2b. The peaks of wüstite and Zn(II) oxide became smaller and the peaks corresponding to the spinel-type compound became larger compared with those obtained in the initial stage (at 1 h). This indicates that the transformation of the slightly oxidized wüstite and Zn(II) oxide into the spinel-type compound proceeds during the second stage of the $CO_2$ decomposition reaction. Therefore, it is considered that the decomposition of the adsorbed CO into carbon takes place by transformation of the slightly oxidized wüstite and Zn(II) oxide into the Zn(II)-bearing ferrite. The lattice constant (0.4311 nm at 1 h) of the slightly oxidized wüstite changed slightly to 0.4309 nm (at 22 h) in the second stage. This change

is small but would cause the reduction of the adsorbed $CO_2$ into the adsorbed CO (Equation 3) in the second stage. This reduction of adsorbed $CO_2$ into adsorbed CO (equation 3) gradually proceeds, accompanying the carbon deposition reaction from the adsorbed CO (Equation 8). From these findings, the reactions including the solid phases will be given by the following equations:
in the second stage

$$Fe_{\delta_2}O + (\delta_2/\delta_3 - 1)CO_2 \rightleftharpoons (\delta_2/\delta_3)Fe_{\delta_3}O + (\delta_2/\delta_3 - 1)CO \quad (\delta_2 > \delta_3) \qquad (11)$$

and

$$Fe_{\delta}O + (\delta/2)ZnO + (3\delta/2 - 1)CO \rightarrow (\delta/2)ZnFe_2O_4 + (3\delta/2 - 1)C \quad (\delta_2 \geq \delta \geq \delta_3) \qquad (12)$$

## 3.2. Decomposition of CO into carbon with the $H_2$-reduced Zn(II)-bearing ferrite

Fig. 4 shows the variation with time of CO and $CO_2$ gas contents ($p$CO, Curve A; and $p$$CO_2$, Curve B) during the reaction between $H_2$- reduced Zn(II)-bearing ferrite and CO gas at 300 °C (the CO decomposition reaction). The initial CO gas content in the reaction cell was 20 kPa. As can be seen from Curve A, the CO content rapidly decreased from about 20 kPa to 10 kPa in 2 h of the initial reaction time. This lowering of the CO content was accompanied by rapid evolution of $CO_2$ gas in the 2 h, as shown by Curve B. As can be seen from Curves A and B, both the rapid CO decrease and the rapid $CO_2$ evolution processes apparently ceased after 2 h of the initial stage of the reaction. This suggests that in the initial stage of the CO decomposition, an equilibrium reaction between the gas phase of the $CO_2$ and CO, and the solid phase, takes place, as given by Equation 1.

As a carbon deposition reaction from CO using iron as a catalyst, the Boudouard reaction, represented by

$$2CO \rightleftharpoons CO_2 + C \qquad (13)$$

is known. However, we cannot apply this reaction to the rapid decrease of CO gas and the rapid evolution of $CO_2$ in the initial stage of the CO decomposition reaction; if the rapid $CO_2$ evolution in the initial reaction time is caused by the Boudouard reaction and the Boudouard reaction attains an equilibrium of an apparent state of rest in the 2 h, the CO gas content initially introduced should decrease nearly to zero and the $CO_2$ of the half volume of the decreased CO gas should be evolved, when considering the equilibrium constant of the Boudouard reaction at 300 °C ($K_p \simeq 10^6$). This assumption is in conflict with the experimental results of Fig. 4: the reaction rate of the Boudouard reaction would be very slow at 300°C.

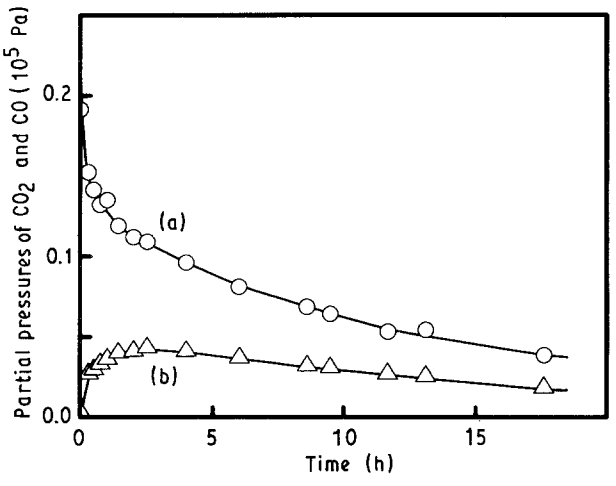


*Figure 4* Variations in the gas contents of (a) CO, and (b) $CO_2$ in the reaction cell as a function of time for the reaction between $H_2$-reduced Zn(II)-bearing ferrite and CO gas at 300 °C. The initial CO gas content in the reaction cell was 20 kPa at 300 °C.

As can be seen from Curve A, in the second stage after the rapid decrease in the CO gas content, the CO gas content gradually decreased with reaction time. At the same time, the $CO_2$ gas content also gradually decreased. The gas content ratio of CO to $CO_2$ gas was kept nearly constant (2:1) during the decrease of the CO and $CO_2$ gas contents. This indicates that the reaction in the second stage of the CO decomposition reaction with $H_2$-reduced Zn(II)-bearing ferrite, proceeds according to the same reaction mechanism as that in the second stage of the $CO_2$ decomposition reaction.

The chemical analysis of the carbon deposited on the solid phase showed that at 18 h reaction time ($p$CO = 4 kPa, and $p$$CO_2$ = 2 kPa at 300 °C) it was about 30% of the carbon of the CO gas initially present in the reaction cell. This amount of deposited carbon was larger than that estimated from the decrease in the evolved $CO_2$ volume (10%), but nearly equal to that estimated from the decreased CO gas volume in the second stage (30%).

Fig. 5 shows the XRD patterns of the solid phases at 3 and 18 h CO decomposition reaction time. As can be seen here, the wüstite and Zn(II) oxide peaks become smaller, and the peaks corresponding to the spinel-type compound appear and become larger (Fig. 5a and b). This indicates that the wüstite and Zn(II) oxide are gradually transformed into the spinel-type compound (Zn(II)-bearing ferrite). However, the lattice constant of the active wüstite ($a_0$ = 0.4319 nm) changed little during the CO decomposition reaction ($a_0$ = 0.4318 nm at 18 h reaction time). Thus the active wüstite was hardly reduced or oxidized into the slightly reduced or oxidized wüstite during the CO decomposition reaction. In the CO decomposition reaction, the reduction of active wüstite with CO in the initial stage (Equation 9), and the oxidation of active wüstite into the slightly oxidized wüstite in the second stage (Equation 11) would proceed only slightly. The main reaction of the CO decomposition reaction with the $H_2$-reduced Zn(II)-ferrite is considered to be the decomposition of the adsorbed CO into carbon accompanying the transformation of the active wüstite and Zn(II) oxide into the Zn(II)-bearing ferrite.

## 4. Conclusions

$CO_2$ gas was decomposed into carbon at 300 °C with the $H_2$-reduced Zn(II)-bearing ferrite in two steps. In

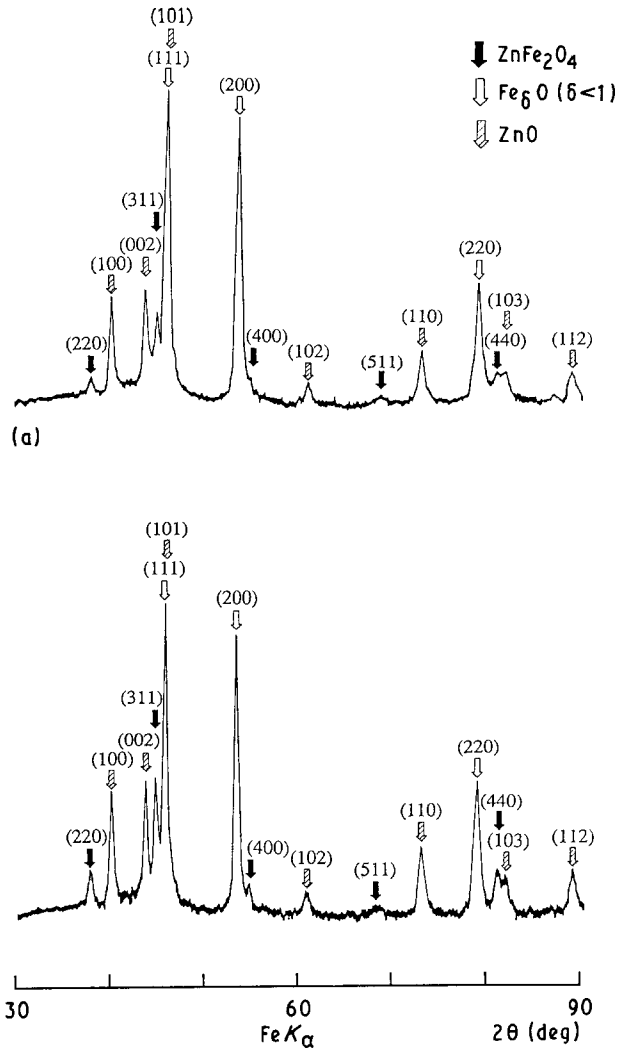


*Figure 5* X-ray diffraction patterns of the solid phases at (a) 3 h and (b) 18 h reaction time between the $H_2$-reduced Zn(II)-bearing ferrite and the CO gas at 300 °C. The initial CO gas content in the reaction cell was 20 kPa at 300 °C.

the initial stage, the reaction of the $H_2$-reduced Zn(II)-bearing ferrite with $CO_2$ gas attains equilibrium of an apparent state of rest between the gas phase of the $CO_2$ and CO, and the solid phase, where the $CO_2$ is reduced to CO. In the initial stage, the reduction of $CO_2$ to CO is accompanied both by oxidation of the active wüstite into the slightly oxidized wüstite and by the transformation of active wüstite and Zn(II) oxide into the Zn(II)-bearing ferrite. After attaining equilibrium of an apparent state of rest in the initial stage, the adsorbed CO is decomposed into carbon, associated with the transformation of the slightly oxidized wüstite and Zn(II) oxide into the Zn(II)-bearing ferrite. On the other hand, CO gas is directly decomposed into carbon, associated with the transformation of the active wüstite and Zn(II) oxide into the Zn(II)-bearing ferrite.

## Acknowledgement

The present work was partially supported by a Grant-in-Aid for Science Research No. 03203216 from the Ministry of Education, Science and Culture.

## References

1. Y. HORI, A. MURATA, K. KIKUCHI and S. SUZUKI, *J. Amer. Chem. Soc.* **109** (1987) 5022.
2. H. NODA, S. IKEDA, Y. ODA, K. IMAI, M. MAEDA and K. ITO, *Bull. Chem. Soc. Jpn.* **63** (1990) 2459.
3. M. ULMAN, A. H. A. TINNEMANS, A. MACKOR, B. AURIAN-BLAJENI and M. HALMANN, *Int. J. Solar Energy* **1** (1982) 213.
4. K. W. FRESE, Jr and D. CANFIELD, *J. Electrochem. Soc.* **131** (1984) 2518.
5. J. HAWECKER, J. LEHN and R. ZIESSEL, *Helv. Chim. Acta* **69** (1986) 1990.
6. J. O'M. BOCKRIS and J. C. WASS, *Mater. Chem. Phys.* **22** (1989) 249.
7. V. A. NAUMOV, *Kinet. Catal.* **22** (1982) 847.
8. J. A. MARCOS, R. H. BUITRAGO and E. A. LOMBARDO, *J. Catal.* **105** (1987) 95.
9. M. A. ULLA, R. A. MIGONE, J. O. PETUNCHI and E. A. LOMBARDO, *ibid.* **105** (1987) 107.
10. M. LEE, J. LEE, C. CHANG and T. DONG, *Appl. Catal.* **72** (1991) 267.
11. A. SACCO, Jr and R. C. REID, *Carbon* **17** (1979) 459.
12. M. LEE, J. LEE and C. CHANG, *J. Chem. Engng Jpn* **23** (1990) 130.
13. "Gmelins Handbuch der Anorganischen Chemie", 8th edn, Kohlenstoff Part C2 (Springer Verlag, Berlin, 1972) p. 203.
14. T. KANZAKI, J. NAKAJIMA, Y. TAMAURA and T. KATSURA, *Bull. Chem. Soc. Jpn* **54** (1981) 135.
15. I. IWASAKI, T. KATSURA, T. OZAWA, M. YOSHIDA, M. MASHIMA, H. HARAMURA and B. IWASAKI, *Bull. Volcanol. Soc. Jpn. Ser. II* **5** (1960) 9.
16. E. R. JETTE and F. FOOTE, *J. Chem. Phys.* **1** (1933) 29.
17. L. S. DARKEN and R. W. GURRY, *J. Amer. Chem. Soc.* **67** (1945) 1945.
18. I. BRANSKY and A. Z. HED, *ibid.* **51** (1968) 231.

*Received 6 January*
*and accepted 11 June 1992*